



RESEARCH ARTICLE

Open Access



Quantitative analysis of an engineered CO₂-fixing *Escherichia coli* reveals great potential of heterotrophic CO₂ fixation

Fuyu Gong^{1,2}, Guoxia Liu¹, Xiaoyun Zhai^{1,2}, Jie Zhou¹, Zhen Cai^{1*} and Yin Li^{1*}

Abstract

Background: Production of fuels from the abundant and wasteful CO₂ is a promising approach to reduce carbon emission and consumption of fossil fuels. Autotrophic microbes naturally assimilate CO₂ using energy from light, hydrogen, and/or sulfur. However, their slow growth rates call for investigation of the possibility of heterotrophic CO₂ fixation. Although preliminary research has suggested that CO₂ fixation in heterotrophic microbes is feasible after incorporation of a CO₂-fixing bypass into the central carbon metabolic pathway, it remains unclear how much and how efficient that CO₂ can be fixed by a heterotrophic microbe.

Results: A simple metabolic flux index was developed to indicate the relative strength of the CO₂-fixation flux. When two sequential enzymes of the cyanobacterial Calvin cycle were incorporated into an *E. coli* strain, the flux of the CO₂-fixing bypass pathway accounts for 13 % of that of the central carbon metabolic pathway. The value was increased to 17 % when the carbonic anhydrase involved in the cyanobacterial carbon concentrating mechanism was introduced, indicating that low intracellular CO₂ concentration is one limiting factor for CO₂ fixation in *E. coli*. The engineered CO₂-fixing *E. coli* with carbonic anhydrase was able to fix CO₂ at a rate of 19.6 mg CO₂ L⁻¹ h⁻¹ or the specific rate of 22.5 mg CO₂ g DCW⁻¹ h⁻¹. This CO₂-fixation rate is comparable with the reported rates of 14 autotrophic cyanobacteria and algae (10.5–147.0 mg CO₂ L⁻¹ h⁻¹ or the specific rates of 3.5–23.7 mg CO₂ g DCW⁻¹ h⁻¹).

Conclusions: The ability of CO₂ fixation was created and improved in *E. coli* by incorporating partial cyanobacterial Calvin cycle and carbon concentrating mechanism, respectively. Quantitative analysis revealed that the CO₂-fixation rate of this strain is comparable with that of the autotrophic cyanobacteria and algae, demonstrating great potential of heterotrophic CO₂ fixation.

Keywords: Carbon fixation, CO₂-fixation rate, Heterotrophic microbe, Carbonic anhydrase, Rubisco

Background

The wasteful greenhouse gas carbon dioxide (CO₂) is a potential raw material for production of chemicals and fuels [1]. To this end, energy input is required since the carbon in CO₂ is in its highest oxidation state. During the past 5 years, a variety of chemicals including ethanol [2–4], *n*-butanol [5–8], acetone [9], isobutyraldehyde [7], lactic acid [10–12], isoprene [13], 1,2-propanediol [14], methane [15], and biodiesel [16, 17] have been produced

from CO₂ by engineered autotrophic microbes such as cyanobacteria and algae, using light as the energy resource. Apart from the light, autotrophic microbes can also use hydrogen and/or sulfur as the energy source for CO₂ assimilation under mild conditions [18].

Heterotrophic microbes usually do not assimilate CO₂ through the central metabolism. Recent studies indicated that incorporation of several steps of a natural carbon fixation pathway into a heterotrophic microbe may create a CO₂-fixing bypass pathway which enables the host to assimilate CO₂ at the expense of carbohydrates. Examples include introduction of two enzymes of Calvin cycle into *Escherichia coli* and *Saccharomyces cerevisiae*,

* Correspondence: caiz@im.ac.cn; yli@im.ac.cn

¹CAS Key Laboratory of Microbial Physiological and Metabolic Engineering, Institute of Microbiology, Chinese Academy of Sciences, No. 1 West Beichen Road Chaoyang District, Beijing 100101, China

Full list of author information is available at the end of the article

which resulted in enhanced CO₂ recycling in an air-tight fermentor [19] and an increased ethanol yield [20], respectively.

Although these preliminary data suggested that heterotrophic CO₂-fixation is feasible, little is done to quantitatively analyze and evaluate the process. To date, simple approaches capable of evaluating the CO₂ flux in heterotrophic microbes are still lacking, since the metabolites of the CO₂-fixing bypass pathway are indistinguishable from those of the central metabolic pathway. Due to lack of quantitative analysis, it remains unclear where the bottleneck for heterotrophic CO₂-fixation is and whether the rate of heterotrophic CO₂-fixation is higher, lower, or comparable with that of autotrophic CO₂-fixation.

The aim of this study was to address the above issues through a quantitative and comprehensive analysis of the heterotrophic CO₂-fixation process. To evaluate the strength of CO₂ flux, a metabolic flux index, MFI_{h-CO₂}, was developed to indicate the metabolic flux ratio between the CO₂-fixing bypass pathway and the central carbon metabolic pathway. The MFI_{h-CO₂} was determined by addition of ¹³C-labeled sodium bicarbonate into the culture medium, followed by quantification of the isotopic-labeled and unlabeled forms of one intracellular metabolite by liquid chromatography–mass spectrometry/mass spectrometry (LC-MS/MS). Comparison of MFI_{h-CO₂} values of several engineered CO₂-fixing *E. coli* strains led to identification of the rate-limiting steps of heterotrophic CO₂ fixation. The strain with the highest MFI_{h-CO₂} value was aerobically cultivated in minimal medium supplemented with xylose in a chamber filled with 5 % CO₂. The mass of fixed CO₂ per liter culture of this strain per hour was calculated by the mass balance of carbon. The CO₂-fixation rate in *E. coli* was then compared with those of several autotrophic microbes to evaluate the potential of heterotrophic CO₂ fixation.

Results

Development of a metabolic flux index, MFI_{h-CO₂}, for relative quantification of heterotrophic CO₂ fixation

It is costly and time-consuming to determine the absolute metabolic flux of CO₂ fixation by quantifying every isotopic-labeled metabolite upon the feed of ¹³CO₂ during cultivation. As the metabolic flux of the central metabolism for a given strain is quite stable, the relative metabolic flux of the CO₂-fixing bypass pathway over that of the central carbon metabolic pathway may give a quantitative understanding on the efficiency of CO₂ fixation. This relative value is then termed as the metabolic flux index of the heterotrophic CO₂-fixation pathway, MFI_{h-CO₂}. At the conjunction of the CO₂-fixing bypass pathway and the central pathway, the metabolite generated by the two pathways can be differentiated by using

¹³C-labeled CO₂ and unlabeled sugar. The amount of the labeled and unlabeled forms of the joint metabolite can be determined and used to calculate the metabolic flux ratio of the two pathways to obtain the MFI_{h-CO₂} value.

Herein, we use a heterotrophic CO₂-fixing *E. coli* strain as a model to elucidate how MFI_{h-CO₂} is calculated. The strain was constructed by incorporating two sequential enzymes in the cyanobacterial Calvin cycle, phosphoribulokinase (PRK), and ribulose-1,5-bisphosphate carboxylase/oxygenase (Rubisco) into the central metabolism of *E. coli*. The incorporated CO₂-fixing bypass pathway starts at ribulose 5-phosphate (Ru5P) in the pentose phosphate pathway of the central metabolism and ends at 3-phosphoglycerate (3PGA) in the glycolysis of the central metabolism (Fig. 1). When the strain is cultured in medium supplemented with ¹³C-labeled sodium bicarbonate, intracellular ¹³CO₂, either generated by diffusion of the extracellular dissolved ¹³CO₂ or by the equilibrium of ¹³C-labeled bicarbonate after its active transportation into cell, will be used as the substrate for Rubisco.

As shown in Fig. 1, we assume *a* mole of 3PGA is generated from the central pathway and *b* mole of ¹³CO₂ is fixed by the Rubisco pathway in a given period of time. Then (*a* + *b*) mole of unlabeled 3PGA and *b* mole of ¹³C-3PGA are generated. At the same period of time, we assume *c* mole of unlabeled 3PGA and *d* mole of ¹³C-3PGA are channeled into the downstream metabolism. It was reported that a small fraction of ¹³C isotope was coupled with all natural ¹²C-containing compounds [21–23]. We then cultivated *E. coli* strains in medium free of any carbon isotope and determined the ratio of ¹³C-3PGA to the unlabeled 3PGA as the basal isotopic level. The ratio was 3.45 % as shown in Additional file 1: Figure S1. We thus assume that 3.45 % of unlabeled 3PGA will convert to its isotopic form. Therefore, the actually detected molar amount of ¹³C-3PGA (*y*) can be calculated by Eq. (1), while the actually detected unlabeled 3PGA (*x*) can be calculated by Eq. (2).

$$y = b + 3.45\% \times (a + b) - d \quad (1)$$

$$x = (1 - 3.45\%) \times (a + b) - c \quad (2)$$

Under a metabolic steady-state, the relationship of *d*, *c*, *x*, and *y* is shown in Eq. (3).

$$d/c = y/x \quad (3)$$

Solution to the equations deduces Eq. (4).

$$\text{MFI}_{\text{h-CO}_2} = b/a = (0.97y - 0.03x)/(1.03x - 0.97y) \quad (4)$$

In this case, only the concentration of ¹³C-labeled and unlabeled 3PGA are required to be determined to calculate the MFI_{h-CO₂}. Compared with quantification of all intracellular isotopic metabolites to calculate the

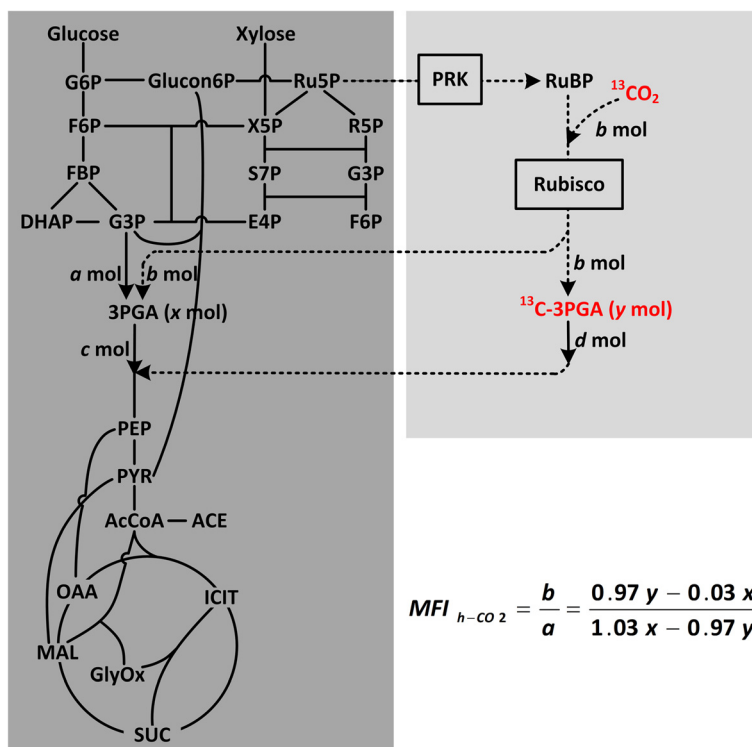


Fig. 1 Metabolic pathway of a CO₂-fixing *E. coli*. The central carbon metabolic pathway is shaded in *dark gray*, while the introduced CO₂-fixation bypass pathway composed of PRK and Rubisco is shaded in *light gray*. The metabolic flux index of heterotrophic CO₂-fixation, MFI_{h-CO₂}, can be calculated by the equation at the bottom right, using the determined amount of unlabeled 3PGA (*x mol*) and ¹³C-labeled 3PGA (*y mol*). 3PGA, 3-phosphoglycerate; AcCoA acetyl-CoA, ACE acetate, DHAP dihydroxyacetone phosphate, E4P erythrose-4-phosphate, F6P fructose-6-phosphate, FBP fructose-1,6-biphosphate, G3P glyceraldehyde-3-phosphate, G6P glucose-6-phosphate, Glucon6P gluconate-6-phosphate, GlyOx glyoxylate, ICIT isocitrate, MAL malate, OAA oxaloacetate, PEP phosphoenolpyruvate, PRK phosphoribulokinase, PYR pyruvate, R5P ribose-5-phosphate, Ru5P ribulose-5-phosphate, Rubisco ribulose-1,5-bisphosphate carboxylase/oxygenase, RuBP ribulose 1,5-bisphosphate, S7P sedoheptulose-7-phosphate, SUC succinate, X5P xylose-5-phosphate

absolute metabolic flux, we argue that the determination of MFI_{h-CO₂} to evaluate the relative metabolic strength of the CO₂-fixation pathway would be a simple and convenient alternative.

Construction of a heterotrophic CO₂-fixing *E. coli*

The Rubisco-encoding genes *rbcL-rbcX-rbcS* from *Synechococcus* sp. PCC7002 and the PRK-encoding gene *prk* from *Synechococcus elongatus* PCC7942 were cloned into pET30a as described previously [24]. The resulted plasmid was designated as pET-RBC-PRK in this study. To verify the function of CO₂-fixation pathway, Rubisco, and/or PRK were deactivated by introducing site-directed mutations to their conserved catalytic residues, yielding another three plasmids, pET-RBC197-PRK, pET-RBC-PRK2021, and pET-RBC197-PRK2021. Among them, RBC197 indicates a K197M mutation in the conserved catalytic site of the large subunit of Rubisco [25], and PRK2021 carries K20M and S21A mutations in the conserved nucleotide-binding sites of ATP-binding proteins [26].

Considerable amount of soluble expression of Rubisco under the T7 promoter was observed in strain BL21(DE3) carrying plasmid pET-RBC-PRK upon IPTG induction (Additional file 1: Figure S2). It was reported that the catalytic product of PRK, ribulose 1,5-bisphosphate, could not be metabolized by *E. coli* and thus caused growth arrest to the cell [24, 27]. Retarded cell growth was indeed seen for strain BL21(DE3)/pET-RBC197-PRK with a deactivated Rubisco (Fig. 2b). Hence, the *prk* gene was leakily expressed without induction of its tryptophan-regulated promoter *trpR*-P_{trp} to avoid severe growth inhibition. It is noteworthy that expression of Rubisco and PRK in *E. coli* BL21(DE3) increased cell growth in the late-phase of induction compared with the strain harboring the empty plasmid pET30a without any gene cloned (Fig. 2b). However, this increase appeared not to be the function of enzymes, as similar increases of growth were also seen in the strains transformed with pET-RBC197-PRK containing the deactivated PRK (Fig. 2b) and pET-RBC197-PRK2021 containing both deactivated enzymes (Additional file 1: Figure S3).

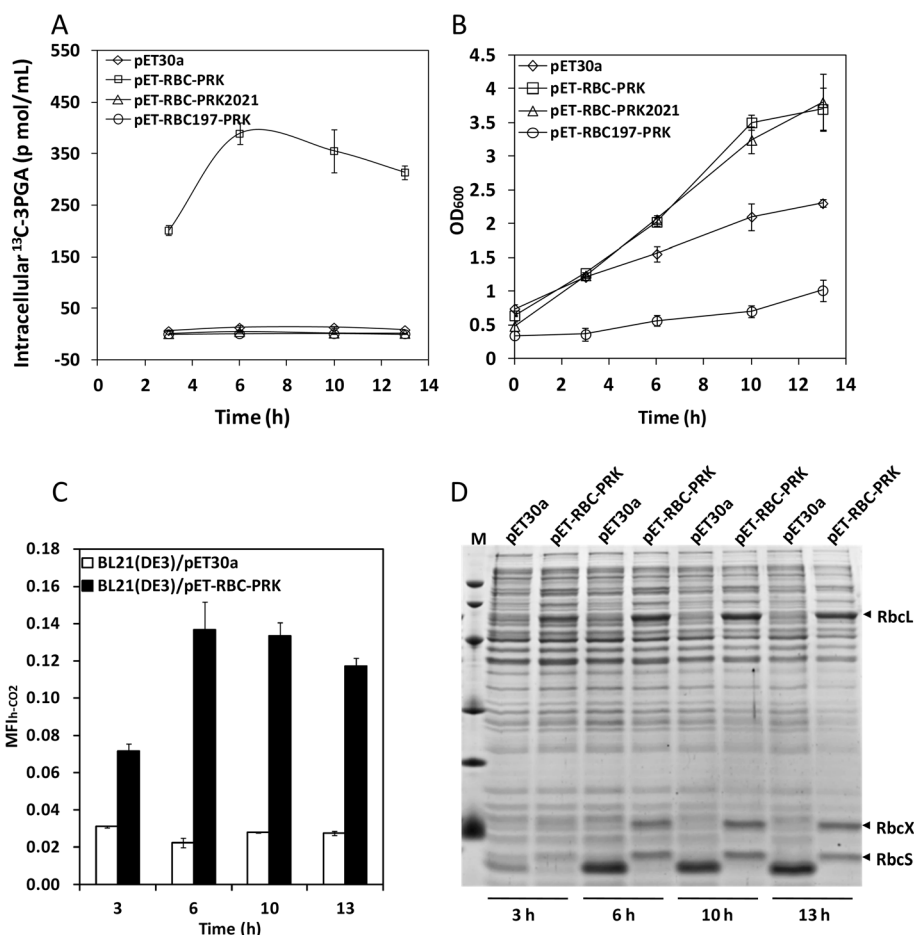


Fig. 2 The intracellular ^{13}C -3PGA (a), cell growth (b), $\text{MFI}_{\text{h-CO}_2}$ values (c), and soluble protein expression (d) of BL21(DE3) strains harboring different plasmids. All strains were 1:100 inoculated into LB medium containing 100 mM $\text{NaH}^{13}\text{CO}_3$ and shaken at 37 °C. When the culture reached the mid-log phase ($\text{OD}_{600} = 0.4\text{--}0.6$), 0.02 mM IPTG was added to induce Rubisco expression and the induction temperature was reduced to 22 °C (zero point). The PRK-encoding gene under the control of a tryptophan-regulated promoter *trpR*- P_{trp} was leakily expressed in LB medium. RbcL and RbcS are the large and small subunits of Rubisco, which are encoded by *rbcL* and *rbcS* genes, respectively. RbcX is the specific chaperon of Rubisco, which is encoded by the *rbcX* gene. Molecular weight standards from top to bottom are 80, 60, 40, 30, 20, and 12 kDa

As shown in Fig. 2a, a significant increase of the ^{13}C -3PGA along with induction time was observed for strain BL21(DE3)/pET-RBC-PRK cultivated with 100 mM $\text{NaH}^{13}\text{CO}_3$. Deactivation of either Rubisco or PRK in strain BL21(DE3)/pET-RBC197-PRK or BL21(DE3)/pET-RBC-PRK2021 decreased the ^{13}C -3PGA production to the basal level of the control strain BL21(DE3)/pET30a. These results clearly demonstrated that the incorporated Rubisco pathway converted CO_2 into 3PGA.

The $\text{MFI}_{\text{h-CO}_2}$ values of strain BL21(DE3)/pET-RBC-PRK at different induction times were calculated to evaluate its relative CO_2 flux (Fig. 2c). For a period of 13 h induction, the $\text{MFI}_{\text{h-CO}_2}$ of the control strain BL21(DE3)/pET30a was below 0.03. Whereas, the $\text{MFI}_{\text{h-CO}_2}$ values of strain BL21(DE3)/pET-RBC-PRK was increased from 0.07 at 3 h to 0.13 at 6 h and then slightly decreased to 0.12 at

13 h. The increase of $\text{MFI}_{\text{h-CO}_2}$ values from 3 to 6 h was associated with the increase of Rubisco expression level (Fig. 2d), suggesting that the increased Rubisco activity contributed to the increased metabolic flux of CO_2 fixation. When protein expression reached a high level from 6 h onwards, the $\text{MFI}_{\text{h-CO}_2}$ also reached its highest value.

Identification of the bottleneck of heterotrophic CO_2 fixation

Rubisco was generally considered as the rate-determining step in the Calvin cycle of autotrophic microbes due to its extremely low catalytic efficiency [28, 29]. For the heterotrophic *E. coli* strain BL21(DE3)/pET-RBC-PRK harboring a partial Calvin cycle, accumulation of RuBP was observed even in the case of leaky-expression of PRK but over-expression of Rubisco. This result suggested that the

Rubisco-catalyzed reaction is one of the rate-limiting steps of the CO₂-fixing bypass pathway in heterotrophic *E. coli* (Additional file 1: Figure S4A). Owing to the difficulty in improving the catalytic activity of Rubisco, we attempted to increase the substrate supply (RuBP or CO₂) for Rubisco to drive the reaction forward.

To increase the supply of RuBP, the weak promoter *trpR*-P_{trp} for PRK expression was replaced by a strong promoter P_{T7}, yielding a plasmid pET-RBC-T7-PRK. A significant increase of PRK expression level and an 8.6-fold increase of intracellular RuBP was observed after promoter replacement (Additional file 1: Figure S4). However, no significant difference in the MFI_{h-CO₂} value (a *P* value of 0.36 using the Student *T* test) was observed after increasing the intracellular RuBP amount (Fig. 3), indicating that RuBP supply was not the rate-limiting factor.

To increase CO₂ supply, the unique cyanobacterial carbon concentrating mechanism (CCM) was introduced into *E. coli*. In cyanobacteria, bicarbonate is first transported to plasma membrane by bicarbonate transporter (BT), diffused into carboxysome, and then converted to CO₂ by carbonic anhydrase (CA) and finally catalyzed by Rubisco therein [30]. To mimic this CCM in *E. coli*, single BT- or CA-encoding gene from *Synechococcus* sp. PCC7002, and their combinations, were respectively introduced into *E. coli*. The *bicA* gene, which encodes a Na⁺-dependent BT with high flux rate [31], was fused with promoter *trpR*-P_{trp} and then inserted into pET-RBC-PRK to generate pET-RBC-PRK-BT. The MFI_{h-CO₂} value of strain BL21(DE3)/pET-RBC-PRK-BT exhibited a decrease of 34.1 % compared with that of strain BL21(DE3)/pET-RBC-PRK (Fig. 3). This can be speculated that the increase of intracellular bicarbonate might cause pH variance and possibly affect expression or function of Rubisco or PRK. Moreover, bicarbonate has to be

converted to CO₂ so as to be catalyzed by Rubisco. The equilibrium of bicarbonate and CO₂ under intracellular condition (e.g., pH 7.5) give the ratio of [HCO₃⁻]/[CO₂] to be 14 (the *pK_a* of H₂CO₃ is 6.35 [32]). The increment of intracellular CO₂ is thus only 7 % of that of bicarbonate. All these indicated that increasing the intracellular bicarbonate by BT expression was not an effective mean to improve heterotrophic CO₂ fixation.

The CA-encoding gene (*ccaA*) was fused with a mutated constitutive bacteriophage promoter P_{L-AA} [33] and then inserted into pET-RBC-PRK and pET-RBC-PRK-BT. The resultant strains BL21(DE3)/pET-RBC-PRK-CA and BL21(DE3)/pET-RBC-PRK-BT-CA showed MFI_{h-CO₂} values of 0.17 and 0.11, respectively, which were 39.8 and 40.7 % higher than those of their respective parent strains without CA insertion (Fig. 3). Overexpression of CA increased the metabolic flux of heterotrophic CO₂-fixation, indicating that CO₂ supply is a limiting factor for CO₂ fixation in *E. coli*.

Determination of the CO₂-fixation rate of the heterotrophic *E. coli*

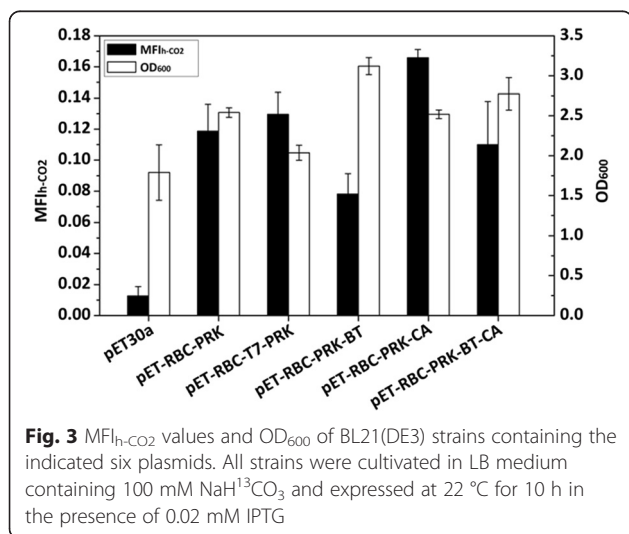
It was reported that *E. coli* metabolized 99 % of the sugar carbon into biomass, CO₂, and acetate under aerobic condition [34]. However, no obvious fermentation product was detected for the CO₂-fixing and control *E. coli* strains after 24 h of aerobic cultivation (Additional file 1: Figure S5). The carbon balance calculation of the control strain BL21(DE3)/pET-RBC197-PRK2021 without the ability of CO₂-fixation also confirmed that the biomass and released CO₂ accounted for 96 % of the consumed sugar carbon. According to the mass balance of carbon, the fixed CO₂ of the CO₂-fixing *E. coli* strain can be calculated by Eq. (5), where all values are in the molar amount of carbon.

$$C_{\text{in fixed CO}_2} = C_{\text{in secreted CO}_2} + C_{\text{in biomass}} - 0.96 \times C_{\text{in consumed sugar}} \quad (5)$$

The specific CO₂ secretion rate of a given *E. coli* is a constant, which was 11.8 mmol g dry weight⁻¹ h⁻¹ reported in one literature [35] and 18.6 mmol g dry weight⁻¹ h⁻¹ in another [34]. Assuming the value is *k*, Eq. (5) can be transformed to Eq. (6).

$$C_{\text{in fixed CO}_2} = (k + 1)C_{\text{in biomass}} - 0.96 \times C_{\text{in consumed xylose}} \quad (6)$$

Mass balance of carbon for the control strain BL21(DE3)/pET-RBC197-PRK2021, which harbored the two deactivated enzymes of the CO₂-fixing pathway, can generate Eq. (7).



$$0.96 \times C_{\text{in consumed xylose}}' = \frac{C_{\text{in secreted CO}_2}'}{+ C_{\text{in biomass}}'} \quad (7)$$

Assuming the specific CO₂ secretion rate of the control strain is k' , Eq. (7) will be transformed to Eq. (8).

$$0.96 \times C_{\text{in consumed xylose}}' = (k' + 1)C_{\text{in biomass}}' \quad (8)$$

Since CO₂ is mainly generated from the tricarboxylic acid cycle of *E. coli* under aerobic conditions, the incorporated CO₂-fixing pathway, which is a bypass of the upstream glycolysis, would not affect the specific CO₂ secretion rate of the strain. Then, under the same cultivation condition, we can assume Eq. (9).

$$k = k' \quad (9)$$

Solution to Eqs. (6), (8), and (9) generates Eq. (10).

$$C_{\text{in fixed CO}_2} = \frac{0.96 \times C_{\text{in consumed xylose}}'}{C_{\text{in biomass}}'} C_{\text{in biomass}} - 0.96 \times C_{\text{in consumed xylose}} \quad (10)$$

Two CO₂-fixing *E. coli* strains and the control strain were aerobically cultivated in 200 mL of M9 minimal medium supplemented with 10 g L⁻¹ xylose in an Erlenmeyer flask. The flask was placed in an air-tight container (10 L) pre-filled with 5 % CO₂ and 95 % air and shaken at room temperature for 24 h. The pH variance, consumed xylose, and generated dry cell weight were determined (Table 1). All cultures maintained a stable pH, with a fluctuation of less than 0.2 unit. Calculation using Eq. (10) indicated that strains BL21(DE3)/pET-RBC-PRK and BL21(DE3)/pET-RBC-PRK-CA were able to fix 13.3 and 19.6 mg CO₂ L⁻¹ h⁻¹, respectively. The 47.4 % of increment in the CO₂-fixation rate after CA expression was similar to the 39.8 % of increment in the MFI_{h-CO2} value, which confirmed that the MFI_{h-CO2} was reliable for evaluating the CO₂-fixation flux in the heterotrophic *E. coli*. The CO₂-fixation rates of the heterotrophic *E. coli* strains constructed in this study were compared with those of the natural CO₂-fixing autotrophic microbes (Table 2). Fourteen autotrophic microbes including microalgae, cyanobacteria, and non-green algae fixed CO₂ at rates ranging from 10.5 to 147.0 mg CO₂ L⁻¹ h⁻¹, with the median value of 21 mg

CO₂ L⁻¹ h⁻¹. The CO₂-fixing *E. coli* strains were able to fix CO₂ at rates of 13.3–19.6 mg CO₂ L⁻¹ h⁻¹, which were comparable to the capacity of the autotrophic microbes.

Discussion

Recycling CO₂ directly into fuels or chemicals is a potential approach to reduce carbon emission as well as to resolve energy crisis [6, 7]. The past 5 years have witnessed great success in production of CO₂-derived molecules that have potential to be used as fuels and chemicals by autotrophic microbes. Quantitative analysis in this study revealed that an engineered heterotrophic *E. coli* could assimilate CO₂ at a rate comparable to that of the autotrophic cyanobacteria and algae. It is noteworthy that the specific CO₂-fixation rates of the *E. coli* strains were superior to most of the autotrophic microbes listed in Table 2. Since *E. coli* can easily grow to a high density in fermentors under well-controlled conditions, we believe that heterotrophic microbes might be an alternative candidate for CO₂ fixation with great potential.

The most striking advantage of using heterotrophic microbes for CO₂ fixation is their fast growth rates. The doubling times for *E. coli* and yeast are only 20 min [36] and 2 h [37], respectively, whereas those for common cyanobacteria and algae are in the range of 8–44 h [38, 39]. Most autotrophic microbes use photosynthesis to provide energy for CO₂ assimilation and ultimately biomass accumulation. The theoretical maximum of solar energy conversion efficiency in photosynthesis is only 8–10 % [40], whereas the actual values for several species of cyanobacteria, microalgae, and plants do not exceed 3 % [41]. The low efficiency of photosynthesis can be ascribed to many inherent factors including insufficient absorption of all light wavelengths during light-dependent reactions and low carboxylation activity of Rubisco and existence of energy-consuming photorespiration during light-independent reactions [42]. Although many efforts have been made [43, 44], dramatic increases in photosynthetic efficiency as well as growth rate are still big challenges for autotrophic microbes [44]. However, billions of years of evolution have enabled the heterotrophic microbes to efficiently assimilate the high-energy sugars to generate both carbon backbone and energy at the same time. Therefore, heterotrophic microbes might be a better

Table 1 The pH variance, consumed xylose, generated biomass, and calculated CO₂-fixation rate of *E. coli* strains after 24 h of aerobic cultivation in 5 % CO₂

Strain	Initial pH	Final pH ^a	Consumed xylose ^a (mmol L ⁻¹)	Biomass ^a (DCW L ⁻¹)	CO ₂ -fixation rate (mg L ⁻¹ h ⁻¹)
BL21(DE3)/pET-RBC-PRK	7.0	6.81 ± 0.06	13.7 ± 1.1	0.82 ± 0.33	13.3 ± 3.2
BL21(DE3)/pET-RBC-PRK-CA	7.0	6.81 ± 0.04	14.8 ± 1.5	0.87 ± 0.29	19.6 ± 4.0
BL21(DE3)/pET-RBC197-PRK2021	7.0	6.87 ± 0.07	29.8 ± 4.7	1.59 ± 0.25	–

^aThe cultivation was independently repeated for three times and the standard deviations were shown after the mean value

Table 2 Comparison of the CO₂-fixation rates of autotrophic and heterotrophic CO₂-fixing microbes

	Species	CO ₂ -fixation rate (mg L ⁻¹ h ⁻¹)	Biomass concentration (g DCW L ⁻¹)	Specific CO ₂ -fixation rate ^a (mg g DCW ⁻¹ h ⁻¹)	CO ₂ concentration (%)	Culture condition	References
Autotrophic microbes							
Microalgae	<i>Chlorella pyrenoidosa</i> SJTU-2	10.8	1.5	7.3	10	1 L flask with 800 mL WW	[52]
	<i>Dunaliella tertiolecta</i> SAD-13.86	11.0	2.1	5.2	10	11 L fermentor with 8 L WW	[53]
	<i>Botryococcus braunii</i> SAG-30.81	21.0	3.1	6.8	10	11 L fermentor with 8 L WW	[53]
	<i>Scenedesmus obliquus</i> SJTU-3	12.1	1.8	6.6	10	1 L flask with 800 mL WW	[52]
	<i>Scenedesmus</i> sp. NIER-10060	25.5	2.7	9.4	15	Photobioreactor	[54]
	<i>Chlorella vulgaris</i> LEB-104	10.5	1.9	5.4	10	11 L fermentor with 8 L WW	[53]
	<i>Chlorella Vulgaris</i> NIER-10003	19.2	1.9	10.2	15	Photobioreactor	[54]
	<i>Chlorella vulgaris</i>	53.0	5.7	9.3	5	Photobioreactor ^c	[55]
Cyanobacteria	<i>Spirulina</i> sp.	17.0 ^a	4.8	3.5	6	2 L vertical tubular photobioreactor with 1.8 L WW	[56]
	<i>Microcystis aeruginosa</i> NIER-10037	20.4	2.3	8.8	15	Photobioreactor	[54]
	<i>Microcystis ichthyoblabe</i> NIER-10040	21.7	2.2	9.8	15	Photobioreactor	[54]
	<i>Anabaena</i> sp. ATCC 33047	60.4	2.7	22.4	0.03 ^b	Glass bubble column photobioreactor	[57]
	<i>Aphanothece microscopica</i>	109.0	5.1	21.4	15	Glass bubble column photobioreactor	[58]
Non-green algae	<i>Phaeodactylum tricornutum</i>	147.0	6.2	23.7	40	Photobioreactor	[59]
Heterotrophic microbes							
Bacteria	<i>E. coli</i> JB	5.8	6.1 ^c	0.95	0.03	3 L fermentor with 1 L WW	[19]
	<i>E. coli</i> BL21(DE3)/PET-RBC-PRK	13.3	0.82	16.2	5	1 L flask with 200 mL WW	This study
	<i>E. coli</i> BL21(DE3)/PET-RBC-PRK-CA	19.6	0.87	22.5	5	1 L flask with 200 mL WW	This study

DCW dry cell weight, WW working volume

^aCalculated by the CO₂-fixation rate in the unit of mg L⁻¹ h⁻¹ divided by the biomass concentration in the unit of g DCW L⁻¹

^bCalculated by multiplying the reported OD₆₀₀ (17.63) by our experimentally determined dry cell weight of *E. coli* (0.35 g L⁻¹ OD₆₀₀⁻¹)

^cSequential photobioreactor using recycle water

choice for CO₂ fixation, since the fixed CO₂ can be easily joined into the central metabolism and then be efficiently metabolized.

For the current version of the CO₂-fixing *E. coli* strain constructed in this study, CO₂ was fixed at the expense of sugar consumption because all energy required for CO₂ fixation comes from sugar. However, it is not unbelievable that CO₂ fixation can occur without sugar consumption in heterotrophic microbes once energy can be supplied from other sources. The pioneer work by Liao's group has demonstrated that electricity can be used as the sole energy to convert CO₂ to higher alcohols in *Ralstonia eutropha* [8], opening the door of employing other energy forms for CO₂ fixation.

There is no doubt that improving the carboxylation activity of Rubisco is the ultimate way to increase the efficiency of CO₂ fixation in both autotrophic and heterotrophic microbes. However, decades of Rubisco engineering gained limited success [24, 45]. In this work, the difficulty of Rubisco in access to CO₂ was found to be another limiting factor of heterotrophic CO₂ fixation. Expression of the CA from *Synechococcus* sp. PCC7002 under a weak constitutive promoter increased the *E. coli* CO₂-fixation rate by 47.4 %. It is thus suggested that screening of the CA gene and optimization of its expression might be feasible ways to further improve the heterotrophic CO₂-fixation rate. CA, which catalyzes the reversible interconversion of CO₂ and HCO₃⁻, is widely existed in animals, plants, archaeobacteria, and eubacteria, and plays an important role in many physiological functions [46]. Although some CAs prefer the direction of CO₂ hydration, the carboxysomal CAs in cyanobacteria and some chemoautotrophic bacteria favor the direction of HCO₃⁻ dehydration. To date, two forms of carboxysomal CAs (α and β), which are encoded by three types of genes with distinct sequences and structures (*CsoSCA* for α -CA and *CcaA* and *CcmM* for β -CA), were reported [47, 48]. The selected CA-encoding gene from *Synechococcus* sp. PCC7002 in this study was the *CcaA* gene. Whether the other two types of CA-encoding genes can be expressed in *E. coli* and whether their expression can increase the heterotrophic CO₂-fixation rate are now under investigation by our group. Moreover, a stronger inducible promoter might be employed to enhance the CA expression in a controllable way to further improve the CO₂ supply.

As a compensation for the low carboxylation activity of Rubisco, some autotrophic microbes have evolved some physical barriers (e.g., the semi-permeable caboxysome in cyanobacteria and the bundle sheath cells in C4 plants) to concentrate CO₂ around Rubisco. Inspired by these, we suppose that constraining CO₂ and the CO₂-fixing enzyme in a microcompartment (e.g., reconstruction of the caboxysome in *E. coli* [49]) or recruiting the

CO₂-producing and CO₂-fixing enzymes in a protein/RNA scaffold in *E. coli* might be an alternative way to further improve its CO₂-fixation rate.

Conclusions

In this study, quantitative analysis approaches have been developed for CO₂ fixation in heterotrophic microbes. The difficulty in access to CO₂ was found to be a limiting factor for heterotrophic CO₂ fixation. An *E. coli* strain capable of fixing CO₂ at a rate of 19.6 mg CO₂ L⁻¹ h⁻¹ or 22.5 mg CO₂ g DCW⁻¹ h⁻¹ was constructed by incorporation of partial cyanobacterial Calvin cycle and carbon concentrating mechanism. This work demonstrated that CO₂ fixation by the engineered heterotrophic *E. coli* can be as effective as the natural autotrophic cyanobacteria and algae, showing great potential of heterotrophic CO₂ fixation.

Methods

Plasmids construction

All plasmids were constructed based on pET30a (Additional file 1: Table S1) and transformed to *E. coli* BL21 (DE3) for protein expression. The primers used are listed in Additional file 1: Table S2.

Isotropic assay for CO₂-fixation efficiency

A fresh single colony of the strain was inoculated into LB medium containing 50 ng μ L⁻¹ kanamycin and cultured overnight at 37 °C. An aliquot of 100 μ L of the overnight culture was inoculated into 40 mL fresh LB medium containing 50 ng μ L⁻¹ kanamycin, 100 mM hydroxyethyl-piperazine ethanesulfonic acid (HEPES), and 100 mM NaH¹³CO₃ (Sigma). The culture was shaken at 37 °C until its OD₆₀₀ reached 0.4–0.6. Then the temperature was reduced to 22 °C for maximal protein expression. At intervals, 3 OD₆₀₀ of cells were harvested for SDS-PAGE and 8 mL of cells for intracellular metabolites extraction.

For SDS-PAGE, 3 OD₆₀₀ of cells were resuspended in 1 mL buffer (100 mM HEPES, pH 8.0, 20 mM MgCl₂, 10 mM KCl, 1 mM EDTA) and sonicated. A 7 μ L aliquot of the supernatant fraction (soluble protein) was subjected to SDS-PAGE (12 % w/v).

For intracellular metabolites extraction, all experiments were done on ice. At first, 10 mL of culture were rapidly centrifuged and washed in 10 mL cold (-20 °C) aqueous methanol solution (60 %, v/v) to quench cell metabolism as soon as possible. The suspension was clarified at -20 °C for 5 min at 20,000g. The cell pellet was resuspended in 80 μ L cold (-20 °C) aqueous methanol solution (60 %, v/v). After addition of 100 μ L of 0.3 M KOH (dissolved in 25 % ethanol), the mixture was stored at -80 °C for more than 2 h to break the cell wall. The alkaline mixture was thawed on ice and neutralized by adding 2 μ L of glacial acetic acid. Then the sample was centrifuged at -20 °C for 10 min at

20,000 g. The supernatant was stored at -80°C before LC-MS/MS detection [50].

LC-MS/MS detection

Agilent 6460 series LC-MS/MS system equipped with a HPLC system and a triple-quadrupole Mass Spectrometer were used. All samples were separated by the reversed phase ion pair high performance liquid chromatography with Agilent XDC18 column (5 μM , 150 mm \times 4.6 mm). The negative ion and selected multiple reactions monitoring (MRM) mode were used for MS detection. Di-*n*-butylammonium acetate (DBAA) was used as the volatile ion pair reagent. DBAA and standard metabolites (3PGA and RuBP) were purchased from Sigma-Aldrich. Methanol was purchased from Fisher Scientific [51]. The mobile phase was the mixture of solution A (water with 5 mM DBAA) and solution B (methanol with 5 mM DBAA) prepared at the gradient shown in Additional file 1: Table S3. The flow rate was 0.6 mL min^{-1} . The injection volume was 50 μL and the column temperature was 40 $^{\circ}\text{C}$.

The settings for MS were as follows: gas temperature, 350 $^{\circ}\text{C}$; gas flow, 8 L min^{-1} ; nebulizer, 38 psi; sheath gas temperature, 350 $^{\circ}\text{C}$; sheath gas flow, 9 L min^{-1} ; capillary, -3500 V ; nozzle voltage, 500 V. The dwell time was set at 200 ms. The MRM parameters were optimized by the standards, and the detailed values for Q1 (m/z of precursor ion), Q3 (m/z of product ion), fragmentor, and collision energy (CE) were listed in Additional file 1: Table S4. All metabolites were quantified by their standard curves.

HPLC detection

The concentrations of xylose in medium before and after cultivation were determined using an Agilent 1200 high performance liquid chromatography (Agilent Technologies, Santa Clara, CA, USA) with a refractive index (RI) detector. An Aminex HPX-87 H organic acid analysis column (7.8 \times 300 mm) (Bio-Rad Laboratories, Inc, CA, USA) was maintained at 15 $^{\circ}\text{C}$ with 0.05 mM sulfuric acid as mobile phase. The injection volume was 10 μL and the flow rate was 0.5 mL min^{-1} .

Additional file

Additional file 1: Tables S1–S5 and Figures S1–S5. Table S1. Plasmids used in this study. **Table S2.** Oligonucleotides used in this study. **Table S3.** Gradient profile of LC-MS/MS. **Table S4.** Optimized parameters of MRM. **Table S5.** Carbon balance of strain BL21(DE3)/pET-RBC197-PRK2021 after 20 h of aerobic cultivation in M9/xylose medium. **Figure S1.** Determination of the basal level of ^{13}C -3PGA which was naturally converted by the unlabeled 3PGA. **Figure S2.** Soluble Rubisco expression of BL21(DE3) strains harboring different plasmids. **Figure S3.** Cell growth for strains BL21(DE3)/pET30a, BL21(DE3)/pET-RBC-PRK, and BL21(DE3)/pET-RBC197-PRK2021. **Figure S4.** The amount of intracellular RuBP (A) and soluble proteins (B) for BL21(DE3) strains harboring plasmids pET30a, pET-RBC-PRK, pET-RBC197-PRK, and pET-RBC-T7-PRK, respectively. **Figure S5.** HPLC detection of fermentation products of different strains at 0 h and 24 h of cultivation.

Abbreviations

Rubisco: ribulose-1,5-bisphosphate carboxylase/oxygenase; PRK: phosphoribulokinase; Ru5P: ribulose 5-phosphate; 3PGA: 3-phosphoglycerate; BT: bicarbonate transporter; CA: carbonic anhydrase; $\text{MFI}_{\text{h-co}_2}$: metabolic flux index of heterotrophic CO_2 fixation; DCW: dry cell weight; LC-MS/MS: liquid chromatography–mass spectrometry/mass spectrometry; MRM: multiple reactions monitoring; DBAA: Di-*n*-butylammonium acetate; HPLC: high performance liquid chromatography.

Competing interests

The authors declare that they have no competing interests.

Authors' contributions

YL developed the concept of this study. FG, GL, XZ, and ZC designed and performed experiments. FG, JZ, ZC, and YL analyzed the data. FG, ZC, and YL wrote the manuscript. All authors read and approved the final manuscript.

Acknowledgements

We would like to thank Zhensheng Xie (Lab of Proteomics, Institute of Biophysics, Chinese Academy of Sciences) for her kind help on the LC-MS/MS and Fitsum Tigu Yifat (Institute of Microbiology, Chinese Academy of Sciences) for his help in revising the manuscript. This work was supported by the National Basic Research Program of China (973 program, 2011CBA00800), National Natural Science Foundation of China (No. 21106175 and 31470231).

Author details

¹CAS Key Laboratory of Microbial Physiological and Metabolic Engineering, Institute of Microbiology, Chinese Academy of Sciences, No. 1 West Beichen Road Chaoyang District, Beijing 100101, China. ²University of the Chinese Academy of Sciences, Beijing, China.

Received: 23 February 2015 Accepted: 5 June 2015

Published online: 18 June 2015

References

- Mikkelsen MJM, Krebs FC. The teraton challenge. A review of fixation and transformation of carbon dioxide. *Energy Environ Sci.* 2010;3:43–81.
- Dexter J, Fu PC. Metabolic engineering of cyanobacteria for ethanol production. *Energy Environ Sci.* 2009;2:857–64.
- Deng MD, Coleman JR. Ethanol synthesis by genetic engineering in cyanobacteria. *Appl Environ Microbiol.* 1999;65:523–8.
- Luo DX, Hu ZS, Choi DG, Thomas VM, Realf MJ, Chance RR. Life cycle energy and greenhouse gas emissions for an ethanol production process based on blue-green algae. *Environ Sci Technol.* 2010;44:8670–7.
- Lan EI, Liao JC. ATP drives direct photosynthetic production of 1-butanol in cyanobacteria. *Proc Natl Acad Sci USA.* 2012;109:6018–23.
- Lan EI, Liao JC. Metabolic engineering of cyanobacteria for 1-butanol production from carbon dioxide. *Metab Eng.* 2011;13:353–63.
- Atsumi S, Higashide W, Liao JC. Direct photosynthetic recycling of carbon dioxide to isobutyraldehyde. *Nat Biotechnol.* 2009;27:1177–80.
- Li H, Opgenorth PH, Wernick DG, Rogers S, Wu TY, Higashide W, et al. Integrated electromicrobial conversion of CO_2 to higher alcohols. *Science.* 2012;335:1596.
- Zhou J, Zhang HF, Zhang YP, Li Y, Ma YH. Designing and creating a modularized synthetic pathway in cyanobacterium *Synechocystis* enables production of acetone from carbon dioxide. *Metab Eng.* 2012;14:394–400.
- Niederholtmeyer H, Wolfstader BT, Savage DF, Silver PA, Way JC. Engineering cyanobacteria to synthesize and export hydrophilic products. *Appl Environ Microbiol.* 2010;76:3462–6.
- Angermayr SA, Pazsota M, Hellingwerf KJ. Engineering a cyanobacterial cell factory for production of lactic acid. *Appl Environ Microbiol.* 2012;78:7098–106.
- Joseph A, Aikawa S, Sasaki K, Tsuge Y, Matsuda F, Tanaka T, et al. Utilization of lactic acid bacterial genes in *Synechocystis* sp PCC 6803 in the production of lactic acid. *Biosci Biotechnol Biochem.* 2013;77:966–70.
- Bentley FK, Melis A. Diffusion-based process for carbon dioxide uptake and isoprene emission in gaseous/aqueous two-phase photobioreactors by photosynthetic microorganisms. *Biotechnol Bioeng.* 2012;109:100–9.
- Li H, Liao JC. Engineering a cyanobacterium as the catalyst for the photosynthetic conversion of CO_2 to 1,2-propanediol. *Microb Cell Fact.* 2013;12:4.

15. Gunther A, Jakob T, Goss R, König S, Spindler D, Rabiger N, et al. Methane production from glycolate excreting algae as a new concept in the production of biofuels. *Bioresour Technol.* 2012;121:454–7.
16. Tang HY, Abunasser N, Garcia MED, Chen M, Ng KYS, Salley SO. Potential of microalgae oil from *Dunaliella tertiolecta* as a feedstock for biodiesel. *Appl Energy.* 2011;88:3324–30.
17. Deng XD, Li YJ, Fei XW. Microalgae: a promising feedstock for biodiesel. *Afr J Microbiol Res.* 2009;3:1008–14.
18. Boyle NR, Morgan JA. Computation of metabolic fluxes and efficiencies for biological carbon dioxide fixation. *Metab Eng.* 2011;13:150–8.
19. Zhuang ZY, Li SY. Rubisco-based engineered *Escherichia coli* for in situ carbon dioxide recycling. *Bioresour Technol.* 2013;150:79–88.
20. Guadalupe-Medina V, Wisselink HW, Luttki MAH, de Hulster E, Daran JM, Pronk JT, et al. Carbon dioxide fixation by Calvin-Cycle enzymes improves ethanol yield in yeast. *Biotechnol Biofuels.* 2013;6:125–36.
21. Friedli H, Lötscher H, Oeschger H, Siegenthaler U, Stauffer B. Ice core record of the $^{13}\text{C}/^{12}\text{C}$ ratio of atmospheric CO_2 in the past two centuries. *Nature.* 1986;324:237–8.
22. Stuiver M, Braziunas TF. Tree cellulose $^{13}\text{C}/^{12}\text{C}$ isotope ratios and climatic change. *Nature.* 1987;328:58–60.
23. Ciais P, Tans PP, Trolier M, White JWC, Francey RJ. A large northern hemisphere terrestrial CO_2 sink indicated by the $^{13}\text{C}/^{12}\text{C}$ ratio of atmospheric CO_2 . *Science.* 1995;269:1098–102.
24. Cai Z, Liu G, Zhang J, Li Y. Development of an activity-directed selection system enabled significant improvement of the carboxylation efficiency of Rubisco. *Protein Cell.* 2014;5:552–62.
25. Cleland WWAT, Gutteridge S, Hartman FC, Lorimer GH. Mechanism of Rubisco: the carbamate as general base. *Chem Rev.* 1998;98:549–62.
26. Higgins CF, Hiles ID, Salmond GP, Gill DR, Downie JA, Evans IJ, et al. A family of related ATP-binding subunits coupled to many distinct biological processes in bacteria. *Nature.* 1986;323:448–50.
27. Parikh MR, Greene DN, Woods KK, Matsumura I. Directed evolution of RuBisCO hypermorphs through genetic selection in engineered *E. coli*. *Protein Eng Des Sel.* 2006;19:1133–9.
28. Robert J, Spreitzer SRP, Satagopan S. Phylogenetic engineering at an interface between large and small subunits imparts land-plant kinetic properties to algal Rubisco. *Proc Natl Acad Sci USA.* 2005;102:17225–30.
29. Parry MA, Andralojc PJ, Mitchell RA, Madgwick PJ, Keys AJ. Manipulation of Rubisco: the amount, activity, function and regulation. *J Exp Bot.* 2003;54:1321–33.
30. Zarzycki J, Axen SD, Kinney JN, Kerfeld CA. Cyanobacterial-based approaches to improving photosynthesis in plants. *J Exp Bot.* 2013;64:787–98.
31. Price GD, Woodger FJ, Badger MR, Howitt SM, Tucker L. Identification of a SulP-type bicarbonate transporter in marine cyanobacteria. *Proc Natl Acad Sci USA.* 2004;101:18228–33.
32. Jn B. Carbon dioxide equilibria and their applications. Michigan, USA: Lewis Publishers Inc; 1991.
33. Alper H, Fischer C, Nevoigt E, Stephanopoulos G. Tuning genetic control through promoter engineering. *Proc Natl Acad Sci USA.* 2005;102:12678–83.
34. Fischer E, Zamboni N, Sauer U. High-throughput metabolic flux analysis based on gas chromatography-mass spectrometry derived C-13 constraints. *Anal Biochem.* 2004;325:308–16.
35. Chen X, Alonso AP, Allen DK, Reed JL, Shachar-Hill Y. Synergy between (^{13}C)-metabolic flux analysis and flux balance analysis for understanding metabolic adaptation to anaerobiosis in *E. coli*. *Metab Eng.* 2011;13:38–48.
36. Bremer H, Dennis PP. Modulation of chemical composition and other parameters of the cell by growth rate. *E Coli Salmonella Cell Mol Biol.* 1996;2:1553–69.
37. Moreno S, Klar A, Nurse P. Molecular genetic analysis of fission yeast *Schizosaccharomyces pombe*. *Methods Enzymol.* 1991;194:795–823.
38. Shastri AA, Morgan JA. Flux balance analysis of photoautotrophic metabolism. *Biotechnol Prog.* 2005;21:1617–26.
39. Griffiths MJ, Harrison STL. Lipid productivity as a key characteristic for choosing algal species for biodiesel production. *J Appl Phycol.* 2009;21:493–507.
40. Hamburger M, Moore GF, Kramer DM, Gust D, Moore AL, Moore TA. Biology and technology for photochemical fuel production. *Chem Soc Rev.* 2009;38:25–35.
41. Melis A. Solar energy conversion efficiencies in photosynthesis: minimizing the chlorophyll antennae to maximize efficiency. *Plant Sci.* 2009;177:272–80.
42. Stephenson PG, Moore CM, Terry MJ, Zubkov MV, Bibby TS. Improving photosynthesis for algal biofuels: toward a green revolution. *Trends Biotechnol.* 2011;29:615–23.
43. Kebeish R, Niessen M, Thiruveedhi K, Bari R, Hirsch HJ, Rosenkranz R, et al. Chloroplastic photorespiratory bypass increases photosynthesis and biomass production in *Arabidopsis thaliana*. *Nat Biotechnol.* 2007;25:593–9.
44. Evans JR. Improving photosynthesis. *Plant Physiol.* 2013;162:1780–93.
45. Whitney SM, Houtz RL, Alonso H. Advancing our understanding and capacity to engineer nature's CO_2 -sequestering enzyme, Rubisco. *Plant Physiol.* 2011;155:27–35.
46. Mitra M, Lato SM, Ynalvez RA, Xiao Y, Moroney JV. Identification of a new chloroplast carbonic anhydrase in *Chlamydomonas reinhardtii*. *Plant Physiol.* 2004;135:173–82.
47. Rae BD, Long BM, Badger MR, Price GD. Functions, compositions, and evolution of the two types of carboxysomes: polyhedral microcompartments that facilitate CO_2 fixation in cyanobacteria and some proteobacteria. *Microbiol Mol Biol Rev.* 2013;77:357–79.
48. Cannon GC, Heinhorst S, Kerfeld CA. Carboxysomal carbonic anhydrases: structure and role in microbial CO_2 fixation. *Biochim Biophys Acta.* 2010;1804:382–92.
49. Bonacci W, Teng PK, Afonso B, Niederholtmeyer H, Grob P, Silver PA, et al. Modularity of a carbon-fixing protein organelle. *Proc Natl Acad Sci USA.* 2012;109:478–83.
50. Luo B, Groenke K, Takors R, Wandrey C, Oldiges M. Simultaneous determination of multiple intracellular metabolites in glycolysis, pentose phosphate pathway and tricarboxylic acid cycle by liquid chromatography-mass spectrometry. *J Chromatogr A.* 2007;1147:153–64.
51. Uematsu K, Suzuki N, Iwamae T, Inui M, Yukawa H. Increased fructose 1,6-bisphosphate aldolase in plastids enhances growth and photosynthesis of tobacco plants. *J Exp Bot.* 2012;63:3001–9.
52. Tang D, Han W, Li P, Miao X, Zhong J. CO_2 biofixation and fatty acid composition of *Scenedesmus obliquus* and *Chlorella pyrenoidosa* in response to different CO_2 levels. *Bioresour Technol.* 2011;102:3071–6.
53. Sydney EB, Sturm W, Carvalho JC, Thomaz-Soccol V, Larroche C, Pandey A, et al. Potential carbon dioxide fixation by industrially important microalgae. *Bioresour Technol.* 2010;101:5892–6.
54. Jin H-F, Lim B-R, Lee K. Influence of nitrate feeding on carbon dioxide fixation by microalgae. *Journal of environmental science and health.* *J Environ Sci Heal A.* 2006;41:2813–24.
55. Lam MKL. Effect of carbon source towards the growth of *Chlorella vulgaris* for CO_2 bio-mitigation and biodiesel production. *Int J Greenhouse Gas Control.* 2013;14:169–76.
56. Morais MG, Costa JA. Carbon dioxide fixation by *Chlorella kessleri*, *C. vulgaris*, *Scenedesmus obliquus* and *Spirulina sp.* cultivated in flasks and vertical tubular photobioreactors. *Biotechnol Lett.* 2007;29:1349–52.
57. Gonzalez Lopez CV, Acien Fernandez FG, Fernandez Sevilla JM, Sanchez Fernandez JF, Ceron Garcia MC, Molina GE. Utilization of the cyanobacteria *Anabaena sp.* ATCC 33047 in CO_2 removal processes. *Bioresour Technol.* 2009;100:5904–10.
58. Jacob-Lopes E, CFLL, Franco TT. Biomass production and carbon dioxide fixation by *Aphanothece microscopica* Nägeli in a bubble column photobioreactor. *Biochem Eng J.* 2008;40:27–34.
59. Mazzuca Sobczuk T, Garcia Camacho F, Camacho Rubio F, Acien Fernandez FG, Molina GE. Carbon dioxide uptake efficiency by outdoor microalgal cultures in tubular airlift photobioreactors. *Biotechnol Bioeng.* 2000;67:465–75.

Submit your next manuscript to BioMed Central and take full advantage of:

- Convenient online submission
- Thorough peer review
- No space constraints or color figure charges
- Immediate publication on acceptance
- Inclusion in PubMed, CAS, Scopus and Google Scholar
- Research which is freely available for redistribution

Submit your manuscript at
www.biomedcentral.com/submit

